Preparation and characterization of sulfur-doped TiO₂/Ti photoelectrodes and their photoelectrocatalytic performance

Haijian Sun, Huiling Liu *, Jun Ma, Xiangyu Wang, Bin Wang, Lei Han

School of Municipal & Environmental Engineering, Harbin Institute of Technology, Harbin 150090, China

Abstract

Sulfur-doped TiO₂/Ti photoelectrodes were prepared by anodization and characterized by SEM, AFM, XRD, XPS, UV–vis and SPS. The results of investigation indicated that S^{4+} and S^{6+} were dispersed on the surface of TiO₂ nanoparticles. The doping with an appropriate amount of sulfur expanded the response range of TiO₂/Ti photoelectrodes to visible light, and enhanced the separation of photoinduced electrons from cavities. The photoelectrocatalytic performance test run with sulfur-doped TiO₂/Ti photoelectrodes under Xenon light indicated that Na_2SO_3 concentration of 750 mg/L and voltage of 160 V were the optimal conditions for preparation of sulfur-doped TiO₂/Ti photoelectrodes.
© 2008 Elsevier B.V. All rights reserved.

Keywords: Sulfur-doped TiO₂/Ti photoelectrode; Anodization; Photocatalytic (PC); Photoelectrocatalytic (PEC) performance

1. Introduction

The good photocatalytic activity, chemical stability and non-toxicity of titanium dioxide (TiO₂) make TiO₂ one of the most promising photocatalysts for the degradation of organic pollutants, but the high energy band gap of pure TiO₂ (3.2 eV) makes it operate effectively as a photocatalyst only when the wavelengths of light is shorter than 387 nm, and thus, it makes use of only a small part of solar light [1,2]. It is therefore of great significance to adjust the band structure of TiO₂ to improve the photoreaction rate.

Much work has been done to improve the photoelectrocatalytic performance of TiO₂ to absorb visible light [3–6], especially by doping with nitrogen and sulfur [7–14]. However, the form of sulfur and the mechanism of doping have not been fully understood yet so far, and so, the influences of chemical valence, content and surface composition of sulfur on the photocatalytic performance of TiO₂, and so on, became the topics of general interest in this particular field in recent years.

Therefore, sulfur-doped TiO₂/Ti photoelectrodes were prepared by anodization for our study [15]. The crystalline component, crystalline grain size, aperture and the content of doped sulfur were controlled using such parameters as current density, voltage and concentration of Na_2SO_3 in the process of anodization to design the function of photoelectrodes. The sulfur-doped TiO₂/Ti photoelectrodes were characterized by SEM, AFM, XRD, XPS, UV–vis and SPS. Rhodamine B (RhB) was employed as reference for photocatalytic (PC) and photoelectrocatalytic (PEC) efficiency under Xenon light irradiation.

2. Experiment

2.1. Materials and instruments

Titanium plate (purity > 99.5%) was purchased from Baoji Titanium and Nickel Manufacturing Ltd. (China). Chemicals were analytical reagent grade and used as supplied.

The samples were characterized by scanning electronic microscopy (SEM), atomic force microscopy (AFM), X-ray diffraction (XRD), X-ray photoelectron spectroscopy (XPS), ultraviolet-visible spectroscopy (UV–vis) and surface photovoltage spectroscopy (SPS). The surface morphology was characterized by D/max-rB SEM. The AFM graphs were made using DI D-3100 AFM (USA). XRD patterns were obtained using a Rigaku D/max-γB diffractometer with Cu Kα radiation ($\lambda = 1.5417$ Å). XPS spectra was generated using PHI 5700
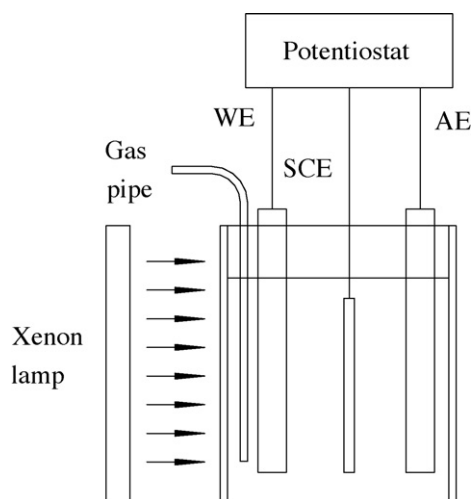
Fig. 1. Schematic diagram of reactor used for PEC oxidation.

Fig. 2. Spectral characteristics of 35 W HID Xenon light.

ESCA system spectrometer with Al Kα source (1486.6 eV). UV–vis spectra in the range of 200–800 nm were recorded using a Lambda 900 UV–vis spectroscope with a diffuse reflectance accessory, and pure TiO_2 was used as references. SPS spectra was generated using the self-made surface photovoltage spectroscope of Jilin University [16,17]. The voltammograms of Sulfur-doped TiO_2/Ti photoelectrodes was mensurated using EG&G 263 electrochemic measuring device.

2.2. Experimental set-up

As shown in Fig. 1, the main components were the cylindrical quartz cell of 25 mm in diameter and 50 mm in height, contains a sulfur-doped TiO_2/Ti photoelectrode, the working electrode (WE) used as the anode, a Pt plate of 50 mm in length and 20 mm in width, the auxiliary electrode (AE) used as the cathode and a saturated calomel electrode (SCE), the reference electrode [18,19]. A 35 W HID Xenon light supplied by Sun Power Company (Germany) was positioned against the reactor facing the sulfur-doped TiO_2/Ti electrode. A YiFei EM1715A potentiostat was used to provide a certain potential bias between the anode and the cathode.

2.3. Preparation of photoelectrodes

Titanium plate was cut into rectangle of 25 mm × 10 mm × 0.5 mm and cleaned in HF (0.54 mol/L) and HNO_3 (0.29 mol/L) mixed at a ratio of 1:1 by volume. The sulfur-doped TiO_2/Ti photoelectrodes were made by anodization in a solution of H_2SO_4 (0.5 mol/L) mixed with Na_2SO_3 concentrations of 250 mg/L, 500 mg/L, 750 mg/L, 1000 mg/L, 1250 mg/L. Titanium and copper plates were used as the anode and cathode, respectively.

Anodization was done in two steps: (1) the current density was kept at 100 mA/cm^2 from the beginning of the oxidation until one of the following voltages (120 V, 140 V, 160 V, 180 V or 200 V) was reached; (2) the voltage of anodization was kept stable until the current density decreased to 36 mA/cm^2. The
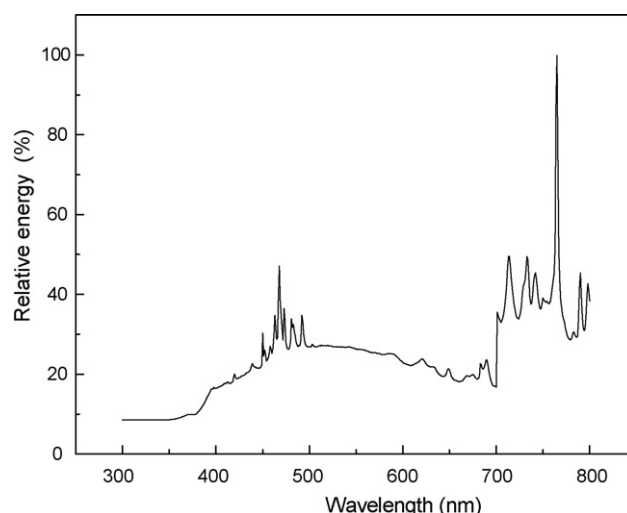
whole anodization process lasted about 10 min. The sulfur-doped TiO_2/Ti electrode was then rinsed in distilled water.

2.4. Degradation of Rhodamine B

15 mL of RhB solution (5 mg/L) was added into the quartz reactor. The freshly prepared sulfur-doped TiO_2/Ti photoelectrode was placed together with a SCE and a Pt plate in the reactor, and connected with the potentiostat to form a typical three-electrode system. The photoelectrocatalytic degradation of RhB was investigated with a potentiostat and 35 W HID Xenon light. The spectral characteristics of 35 W HID Xenon light shown in Fig. 2 was obtained using a GCK-1 Ray radiation automatic control meter. Air was pumped into the reactor through a gas pipe to mix with the solution. The degradation of RhB was analyzed using a 752 spectrophotometer at 552 nm.
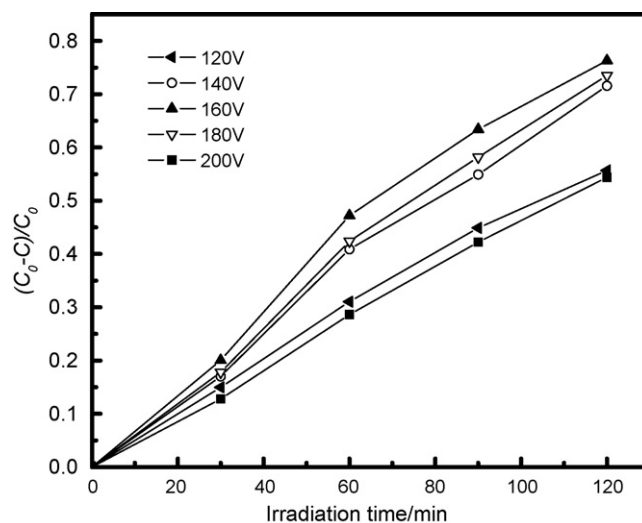

Fig. 3. Effect of electrolysis voltage on PC oxidation performance of sulfur-doped TiO_2/Ti photoelectrodes.
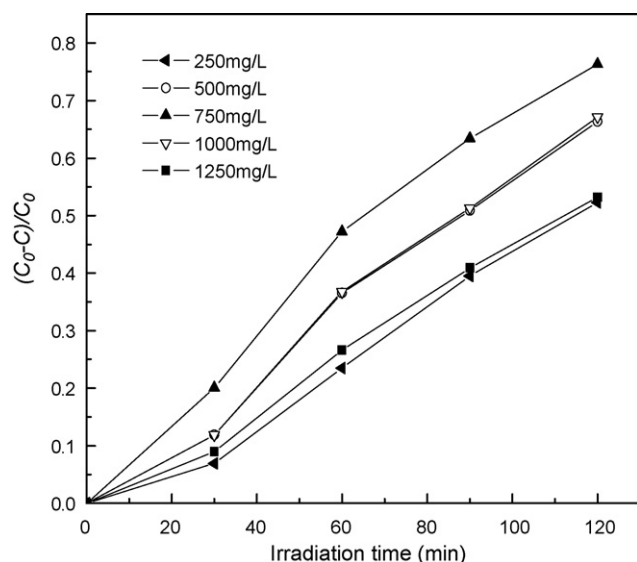
Fig. 4. Effect of Na$_2$SO$_3$ concentration on PC oxidation performance of sulfur-doped TiO$_2$/Ti photoelectrodes.

The degradation of RhB:

$$D\,(\%) = \frac{C_0 - C}{C_0} \times 100\%$$

where C_0 is the initial concentration; C is the concentration after a certain period of illumination time.

3. Results and discussion

3.1. Photocatalytic (PC) oxidation performance

Sulfur-doped TiO$_2$/Ti photoelectrodes were prepared at different electrolysis voltages of 120 V, 140 V, 160 V, 180 V and 200 V, and a Na$_2$SO$_3$ concentration of 750 mg/L. As shown in Fig. 3, the PC performance of sulfur-doped TiO$_2$/Ti photoelectrodes is its best at 160 V. The degradation rate of RhB gradually increases with the electrolysis voltage when the electrolysis voltage is below 160 V. The photoactivity of sulfur-doped TiO$_2$/Ti photoelectrodes gradually decreases as the electrolysis voltage approaches 200 V when the electrolysis voltage is above 160 V. This means that an excessive electrolysis voltage may change

Table 1
Anodization parameters of sulfur-doped TiO$_2$/Ti photoelectrodes

Time (min)	Electrode sample			
	PureTiO$_2$/Ti photoelectrodes		Sulfur-doped TiO$_2$/Ti photoelectrodes	
	Current density (mA/cm^2)	Voltage (V)	Current density (mA/cm^2)	Voltage (V)
1.0	100	30	100	25
2.0	100	60	100	50
3.0	100	90	100	75
4.0	100	120	100	100
5.0	100	160	100	125
6.0	86	160	100	150
7.0	62	160	100	160
8.0	36	160	88	160
9.0	36	160	66	160
1.0	36	160	36	160

the crystal structure of anatase TiO$_2$ to that of rutile TiO$_2$, so that the PC oxidation performance of TiO$_2$ deteriorates.

Sulfur-doped TiO$_2$/Ti photoelectrodes were prepared at different Na$_2$SO$_3$ concentrations of 250 mg/L, 500 mg/L, 750 mg/L, 1000 mg/L, 1250 mg/L and voltage of 160 V. As shown in Fig. 4, the PC performance of sulfur-doped TiO$_2$/Ti photoelectrodes is the best at the Na$_2$SO$_3$ concentration of 750 mg/L. The degradation rate of RhB gradually increases with the concentration of Na$_2$SO$_3$ when the Na$_2$SO$_3$ concentration is below 750 mg/L. The photoactivity of sulfur-doped TiO$_2$/Ti photoelectrodes gradually decreases until the Na$_2$SO$_3$ of reaches 1250 mg/L when the Na$_2$SO$_3$ concentration is above 750 mg/L. This means that the excessive doping of sulfur may make the sulfur become center for the recombination of photoinduced electrons and cavities so that the PC oxidation performance of TiO$_2$/Ti photoelectrodes deteriorated. It is therefore concluded that the Na$_2$SO$_3$ concentration of 750 mg/L and the voltage of 160 V are the optimal conditions for preparation of TiO$_2$/Ti photoelectrodes.

A comparative experiment was run with the TiO$_2$/Ti photoelectrodes we previously prepared at 160 V [2]. It can be seen from Table 1 that at the Na$_2$SO$_3$ concentration of 750 mg/L, it takes longer to reach the voltage of 160 V. The results of
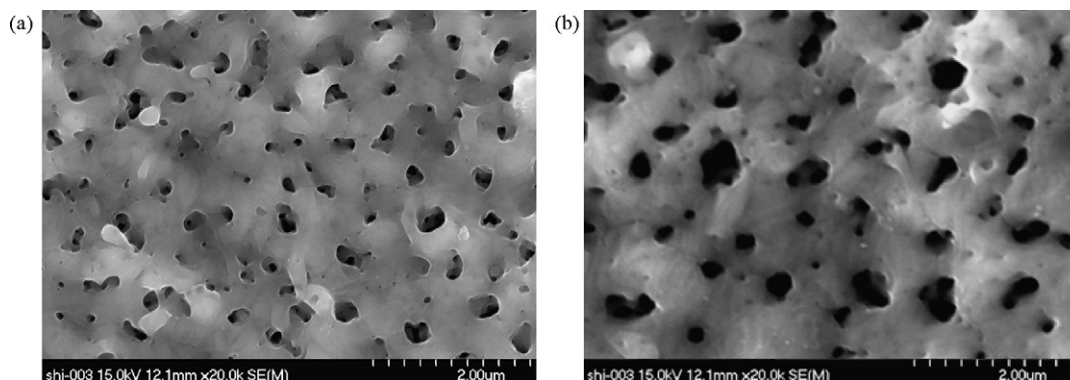

Fig. 5. SEM images of photoelectrodes: (a) sulfur-doped TiO$_2$/Ti photoelectrodes and (b) TiO$_2$/Ti photoelectrodes.
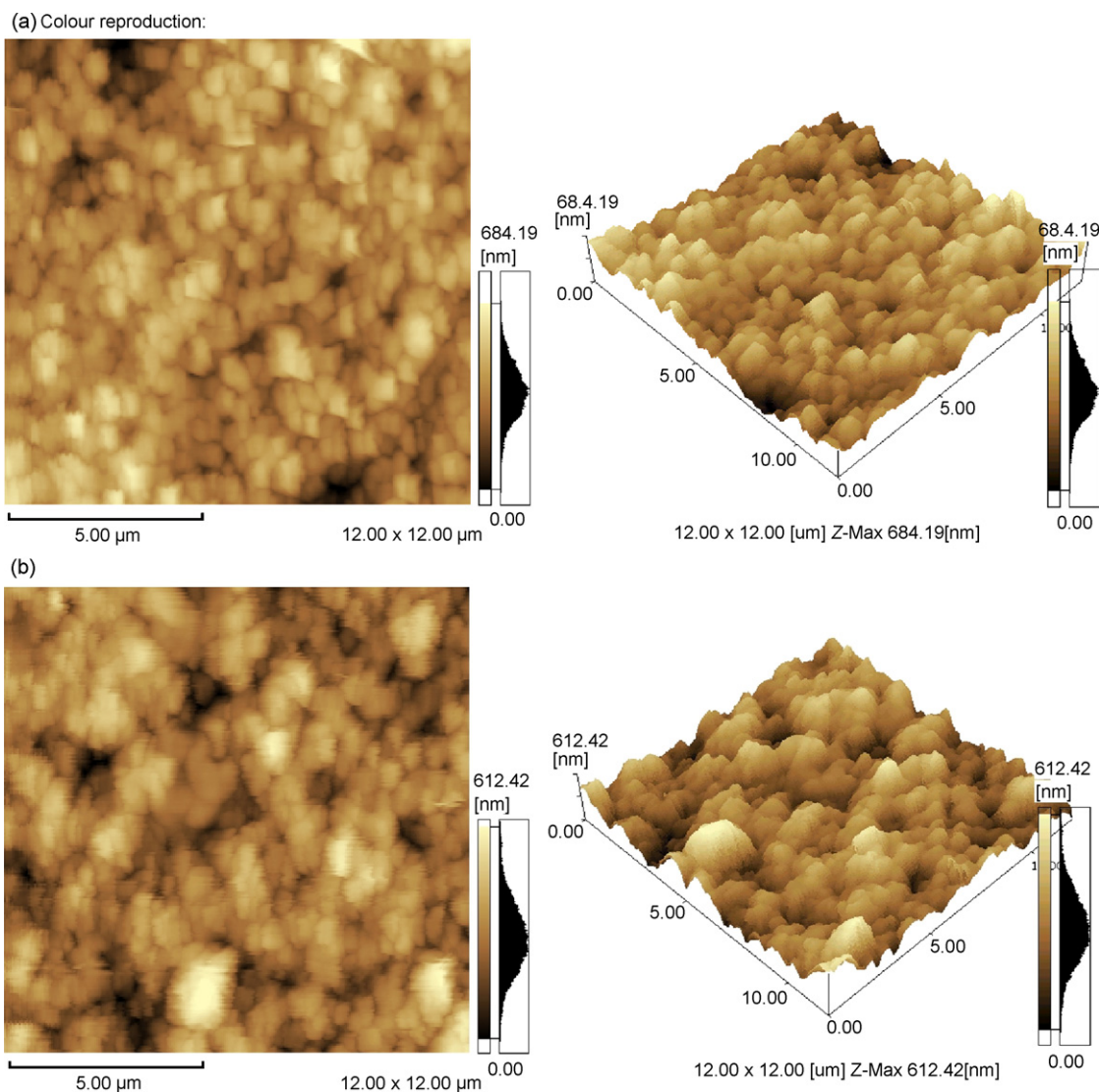
Fig. 6. AFM graphs of photoelectrodes: (a) sulfur-doped TiO$_2$/Ti photoelectrodes and (b) TiO$_2$/Ti photoelectrodes.

investigation by SEM and AFM indicated that the morphology of sulfur-doped TiO$_2$/Ti photoelectrodes varies with anodization parameters.

3.2. Analyses by SEM and AFM

The examination of photoelectrodes by SEM and AFM indicated that the size of the micropore in the sulfur-doped TiO$_2$/Ti photoelectrodes ranged from 40 nm to 200 nm (Fig. 5(a))

and the size of the micropore in the TiO$_2$/Ti photoelectrodes ranged from 40 nm to 400 nm (Fig. 5(a)). It can therefore be concluded that the micropore in the sulfur-doped TiO$_2$/Ti photoelectrode was smaller in size than that in the TiO$_2$/Ti photoelectrode.

The roughness values of sulfur-doped TiO$_2$/Ti and TiO$_2$/Ti photoelectrodes obtained by AFM were 106.9 nm and 92.5 nm, respectively (Fig. 6). This means that specific area of increased after sulfur was doped into TiO$_2$/Ti photoelectrodes. The average

Table 2
Lattice parameters of sulfur-doped TiO$_2$/Ti photoelectrodes

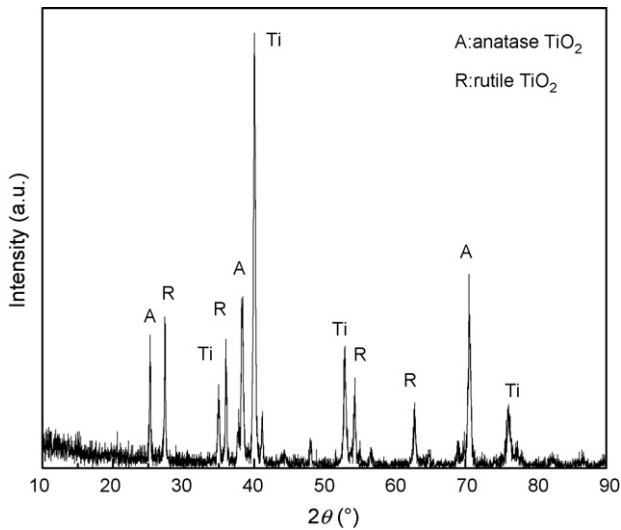| Electrode sample	Main preparation parameters		Lattice parameters		
	Voltage (V)	NaSO$_3$ concentration (mg/L)	a (nm)	c (nm)	Cell volume (nm^3)
Pure TiO$_2$/Ti	160	0	0.3785	0.9514	0.1363
Sulfur-	160	250	0.3729	1.0029	0.1395
doped	160	750	0.3776	0.9843	0.1403
TiO$_2$/Ti	160	1250	0.3778	0.9745	0.1391

Fig. 7. XRD pattern of sulfur-doped TiO_2/Ti photoelectrodes.

particle sizes of sulfur-doped TiO_2/Ti and TiO_2/Ti photoelectrodes were 200 nm and 300 nm, respectively. Moreover, the particle size of sulfur-doped TiO_2/Ti photoelectrodes was much smaller than that of TiO_2/Ti photoelectrodes.

The morphology of sulfur-doped TiO_2/Ti photoelectrodes had obviously been changed, because the anodization was delayed by the Na_2SO_3 concentration of 750 mg/L. The particle size of sulfur-doped TiO_2/Ti photoelectrode was more homogenenous than that of pure TiO_2/Ti photoelectrode.

3.3. Analysis by XRD

It can be seen form the XRD pattern shown in Fig. 7 that anatase TiO_2 of crystal TiO_2 was 62.9%; the diffracted angles (2θ) were 25.28, 38.57, 70.30 and belonged to the (1 0 1), (1 1 2), (2 2 0) diffraction peaks, respectively. The crystalline granule diameter of sulfur-doped TiO_2/Ti photoelectrodes obtained using Scherre formula was 70 nm. The crystal diameter of the sulfur-doped TiO_2/Ti photoelectrodes was finer than crystal diameter (150 nm) of TiO_2/Ti photoelectrode. The results of AFM and XRD indicated that the sulfur-doped TiO_2/Ti photoelectrodes had obviously an aggregate structure.

In addition, the lattice parameters of TiO_2 photoelectrodes tabulated in Table 2 indicated that lattice was expanded after sulfur was doped into TiO_2 lattice. The doping of sulfur led to distortion of TiO_2 lattice and induced more lattice defects. These defects became the centers for recombination of photoinduced electrons and cavities. The results tabulated in Table 2 indicated that the Na_2SO_3 concentration of 750 mg/L led to further expansion of lattice cell and more lattice defects in TiO_2. In addition, we found through experiments that the sulfur-doped TiO_2/Ti photoelectrodes had a very good PEC effect at this time. So, it is logic to say that the change in the volume of a
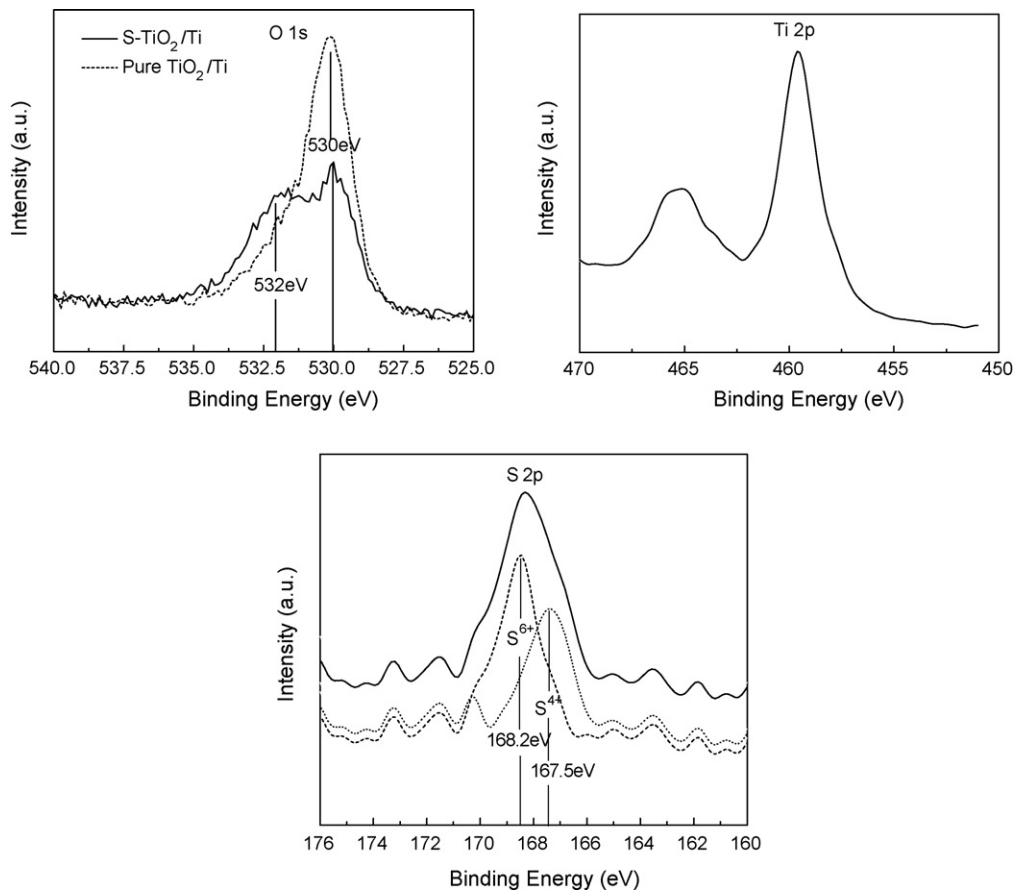

Fig. 8. XPS spectra of O 1s, Ti 2p and S 2p of sulfur-doped TiO_2/Ti photoelectrodes.

cell had its influence on the PEC effect of sulfur-doped TiO$_2$/Ti photoelectrodes.

3.4. Analysis by XPS

As shown in Fig. 8, the XPS spectra of O 1s was asymmetric compared to that of pure TiO$_2$/Ti photoelectrodes, which means at least two kinds of oxygen species were on the surface. The dominant peak at about 530 eV was the characteristic peak of metallic oxides, which was in agreement with O 1s electron binding energy arising from the titania lattice. The oxygen atoms in the titania matrix made the primary contribution to the spectrum. Another O 1s peak at 532 eV was due to the surface hydroxyl, which had an important effect on the PEC reaction [20,21]. From the XPS spectra of O 1s, the surface hydroxyl content in the sulfur-doped TiO$_2$/Ti photoelectrode was higher than that in the pure TiO$_2$/Ti photoelectrode. Consequently the sulfur doping could promote the adsorption of surface hydroxyl. Surface hydroxyl could capture photoinduced cavities and form hydroxy free radical. Because hydroxy free radical was better oxidant, oxidation reaction could easily take place in solution. Therefore, sulfur doping had its influence on the state of O 1s and improved the PEC efficiency of sulfur-doped TiO$_2$/Ti photoelectrodes. From the Ti 2p XPS spectra of sulfur-doped TiO$_2$/Ti photoelectrodes, the spin-orbit components (2p$_{3/2}$ and 2p$_{1/2}$) of the peak were well deconvoluted by two curves at approximately 458.5 eV and 464.2 eV, respectively, which indicated that the Ti elements mainly existed in the chemical state of Ti^{4+} [22,23]. It seemed that the sulfur doping did not have any effect on the position of Ti 2p peak.

The S 2p XPS spectra had a superposed absorption peak at approximately 168.2 eV and 167.5 eV, respectively. The peak seemed to consist of several oxidation states of S atoms such as S^{6+} and S^{4+} states. The peak of 168.2 eV was S^{6+} absorption peak and the peak of 167.5 eV was S^{4+} absorption peak [24,25]. The results of investigation indicated that sulfur was dispersed over the TiO$_2$ nanoparticles with the chemical states of S^{4+} and S^{6+}. Because the state of S^{6+} could easily get electrons and change into the state of S^{4+} in the process of PEC, the state of S^{6+} became the center for capture of photoinduced electrons and the state of S^{4+} became the center for capture of photoinduced cavities; which effectively controlled the recombination of photoinduced electrons and cavities. Consequently, the PEC effect of sulfur-doped TiO$_2$/Ti photoelectrodes was improved.

3.5. Analysis by UV–vis and SPS

As shown in Fig. 9, the sulfur doping obviously absorbed UV light, and extended the range of absorbing wavelength to 425 nm and had a little response on 525 nm.

As shown in Fig. 8, the sulfur-doped TiO$_2$/Ti photoelectrode obviously had a SPS signal, which corresponded to the electronical transition of TiO$_2$ [26]. The doped sulfur weakened the SPS signal of TiO$_2$ nanoparticles. Compared to the sample testing result, that photocatalytic activity increased with the weakening of SPS signal. As shown in Fig. 10, the doped sulfur extended the range of absorption wavelength into the range of visible
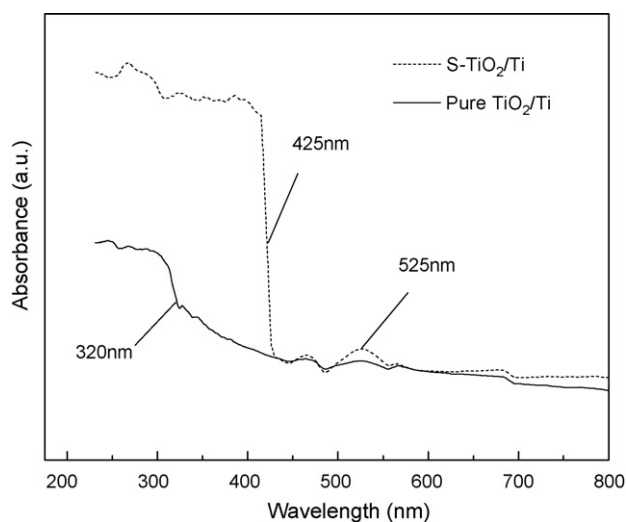
Fig. 9. UV–vis absorption spectra of sulfur-doped TiO$_2$/Ti photoelectrodes.

light and improved the utilization of visible light. This result coincided well with UV–vis absorption spectra.

3.6. Effect of potential bias

In order to select an appropriate potential bias, linear sweep voltammetry was performed for PEC oxidation of RhB solution. As shown in Fig. 11, that under 35 W Xenon light, the anodic photocurrent increased initially with potential bias and then reached saturation. When the anodic potential bias went beyond +1.0 V, the photocurrent seemed to approach the limiting value for a higher potential bias. Thus the potential bias of +1.0 V was selected for PEC experiment.

The result of investigation indicated the potential bias could bend the structure of TiO$_2$ energy band, promote the separation of photoinduced current carriers, and decrease the simple recombination rate of the electrons and holes [27]. The degradation of PEC oxidation RhB could be improved when the simple recombination rate of electrons and cavities decreased
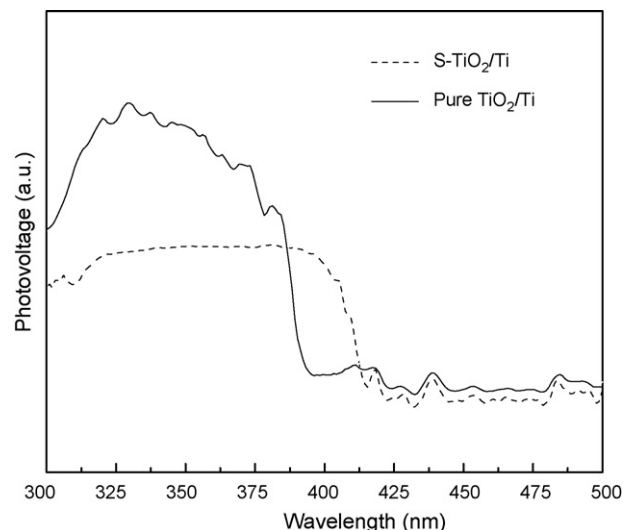
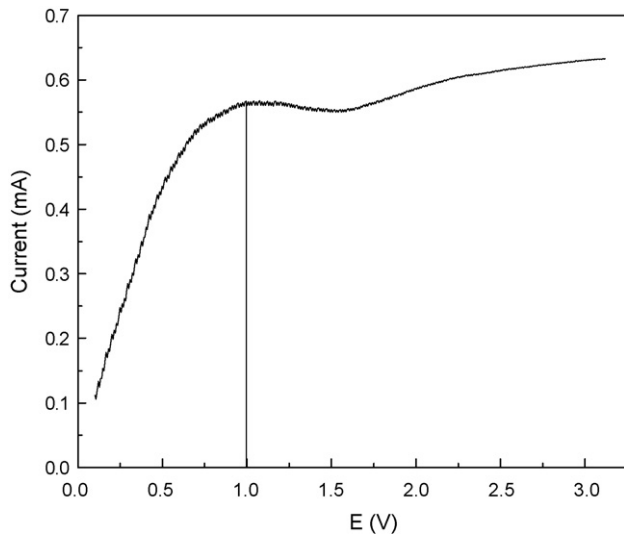Fig. 10. SPS spectra of sulfur-doped TiO$_2$/Ti photoelectrodes.

Fig. 11. Voltammograms of sulfur-doped TiO$_2$/Ti photoelectrodes.

Fig. 13. Lifespan of sulfur-doped TiO$_2$/Ti photoelectrodes.

and the number of photoinduced current carriers increased with the increase of potential bias. The number of photoinduced current carriers was fixed when the light intensity was fixed. When potential bias reached a certain value, the photoinduced current carriers and the cavities totally separated from each other and formed a saturated light current, even when the potential bias was increased, the degradation of RhB was not obviously improved.

3.7. PEC oxidation performance

The sulfur-doped TiO$_2$/Ti photoelectrodes were used for PEC oxidation RhB solution under Xenon light. PEC effect was preferable with a potential bias of +1.0 V [28–30]. In a comparative experiment, TiO$_2$/Ti photoelectrodes were prepared at 160 V with a preferable potential bias of +0.6 V [2]. As shown in Fig. 12, the PC and PEC efficiencies of sulfur-doped TiO$_2$/Ti
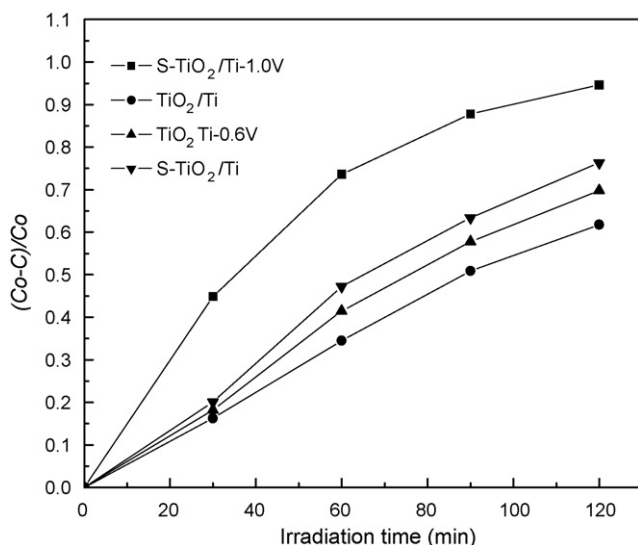

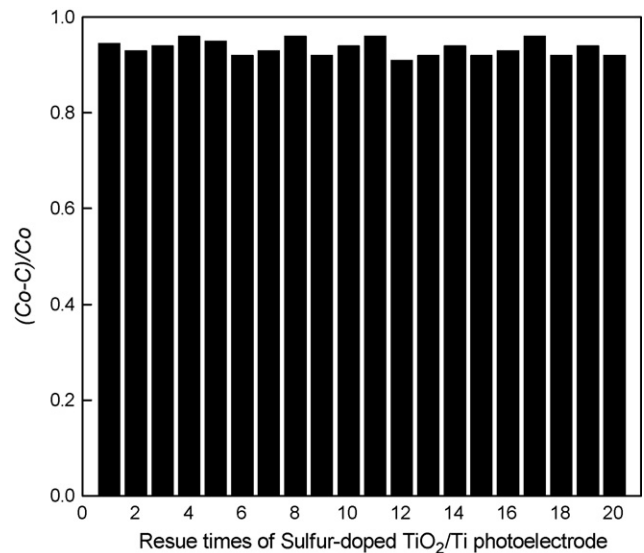Fig. 12. PEC oxidation performance of sulfur-doped TiO$_2$/Ti and TiO$_2$/Ti photoelectrodes.

photoelectrodes increased by 14.53% and 24.76%, respectively compared to those of TiO$_2$/Ti photoelectrodes (Fig. 13).

3.8. The lifespan of sulfur-doped TiO$_2$/Ti photoelectrode

The sulfur-doped TiO$_2$/Ti photoelectrodes were used for PEC oxidation RhB solution under Xenon light with a potential bias of +1.0 V. The sulfur-doped TiO$_2$/Ti photoelectrodes could be used for about 20 times. The PEC performance of sulfur-doped TiO$_2$/Ti photoelectrodes was not obviously deteriorated after these electrodes were used for about 20 times. This was indication of that the sulfur-doped TiO$_2$/Ti photoelectrodes had a longer lifespan and a very good stability performance.

4. Conclusions

The Na$_2$SO$_3$ concentration of 750 mg/L and the voltage of 160 V are the optimal conditions for preparation of sulfur-doped TiO$_2$/Ti photoelectrodes. The anatase TiO$_2$ of sulfur-doped TiO$_2$/Ti photoelectrodes was 62.9% of crystal TiO$_2$. The diameter of TiO$_2$ nanoparticles was 70 nm. S^{4+} and S^{6+} were dispersed on the TiO$_2$ nanoparticles. The properly doped sulfur led to more lattice cell expansion and lattice defects, which enhanced the separation efficiency of photoinduced electrons and cavities. Surface hydroxyls could capture photoinduced cavities and form hydroxy free radicals. Sulfur-doped TiO$_2$/Ti photoelectrodes could be used as a photoelectrocatalyzer to increase the degradation efficiency of RhB because hydroxy free radicals were better oxidants.

References

[1] A. Fujishima, K. Honda, Electrochemical photocatalysis of water at a semiconductor electrode, Nature 238 (1972) 37–38.

[2] X.Z. Li, H.L. Liu, P.T. Yue, Y.P. Sun, Photoelectrocatalytic oxidation of rose bengal in aqueous solution using a Ti/TiO$_2$ mesh electrode, Environ. Sci. Technol. 34 (2000) 4401–4406.

[3] H. Tokudome, M. Miyauchi, N-doped TiO$_2$ nanotube with visible light activity, Chem. Lett. 33 (2004) 1108–1109.

[4] S.W. Yang, L. Gao, Simple and effective preparation of N-doped TiO$_2$ nanocrystallites with visible-light activities, J. Inorgan. Mater. 20 (2005) 785–788.

[5] S. Sato, R. Nakamura, S. Abe, Visible-light sensitization of TiO$_2$ photocatalysts by wet-method N doping, Appl. Catal. Gen. A 284 (2005) 131–137.

[6] H.J. Sun, H.L. Liu, Preparation of cerium-doped TiO$_2$/Ti photoelectrods and photoelectrocatalytic performance under visible light, J. Inorgan. Mater. 22 (2007) 1065–1069.

[7] S.Z. Chen, P.Y. Zhang, W.P. Zhu, F.D. Liu, Progress in visible light responding photocatalysts, Prog. Chem. 16 (2004) 613–619.

[8] R. Bacsa, J. Kiwi, T. Ohno, P. Albers, V. Nadtochenko, Preparation, testing and characterization of doped TiO$_2$ active in the peroxidation of biomolecules under visible light, J. Phys. Chem. B 109 (2005) 5994–6003.

[9] S. Yin, Y. Aita, M. Komatsu, J.S. Wang, Q. Tang, T. Sato, Synthesis of excellent visible-light responsive TiO$_2$–xN$_y$ photocatalyst by a homogeneous precipitation-solvothermal process, J. Mater. Chem. 15 (2005) 674–682.

[10] D. Li, H. Haneda, S. Hishita, N. Ohashi, Visible-light-active nitrogen-containing TiO$_2$ photocatalysts prepared by spray pyrolysis, Res. Chem. Intermed. 31 (2005) 331–341.

[11] Q.W. Zhang, J. Wang, S. Yin, T. Sato, F. Saito, Synthesis of a visible-light active TiO$_2$–xS$_x$ photocatalyst by means of mechanochemical doping, J. Am. Ceram. Soc. 87 (2004) 1161–1163.

[12] T. Ohno, T. Mitsui, M. Matsumura, Photocatalytic activity of S-doped TiO$_2$ photocatalyst under visible light, Chem. Lett. 32 (2003) 364–365.

[13] T. Ohno, Preparation of visible light active S-doped TiO$_2$ photocatalysts and their photocatalytic activities, Water Sci. Technol. 49 (2004) 159–163.

[14] T. Umebayashi, T. Yamaki, S. Tanaka, K. Asai, Visible light-induced degradation of methylene blue on S-doped TiO$_2$, Chem. Lett. 32 (2003) 330–331.

[15] H.Y. Liu, L. Gao, S-doped rutile TiO$_2$ visible-light activated photocatalyst by in situ wet chemical synthesis method, J. Inorgan. Mater. 20 (2005) 470–474.

[16] K.Y. Li, D.J. Wang, F.Q. Wu, T.F. Xie, T.J. Li, Surface electronic states and photovoltage gas-sensitive characters of nanocrystalline LaFeO$_3$, Mater. Chem. Phys. 64 (2000) 269–272.

[17] X.M. Qian, D.Q. Qin, Q. Song, Y.B. Bai, T.J. Li, X.Y. Tang, E.K. Wang, S.J. Dong, Surface photovoltage spectra and photoelectrochemical properties of semiconductor-sensitized nanostructured TiO$_2$ electrodes, Thin Solid Films 385 (2001) 152–161.

[18] J.Q. Li, L. Zheng, L.P. Li, Y.Z. Xian, L.T. Jin, Fabrication of TiO$_2$/Ti electrode by laser-assisted anodic oxidation and its application on photoelectrocatalytic degradation of methylene blue, J. Hazard. Mater. 139 (2007) 72–78.

[19] W.H. Leng, Z. Zhang, J.Q. Zhang, C.N. Cao, Investigation of the kinetics of a TiO$_2$ photoelectrocatalytic reaction involving charge transfer and recombination through surface states by electrochemical impedance spectroscopy, J. Phys. Chem. 109 (2005) 15008–15023.

[20] M.R. Hoffmann, S.T. Martin, W.Y. Choi, D.W. Bahnemann, Environmental applications of semiconductor photocatalysis, Chem. Rev. 95 (1995) 69–96.

[21] Q.N. Zhao, C.L. Li, X. He, X.J. Zhao, XPS study of N-doped TiO$_x$ thin films prepared by DC reactive magnetron sputtering, Comp. Mater. III Key Eng. Mater. 249 (2003) 457–461.

[22] J. Biener, M. Baumer, J. Wang, R.J. Madix, Electronic structure and growth of vanadium on TiO$_2$ (1 1 0), Surf. Sci. 450 (2000) 12–26.

[23] Q.G. Wang, R.J. Madix, Preparation and reactions of V$_2$O$_5$ supported on TiO$_2$ (1 1 0), Surf. Sci. 474 (2001) 213–216.

[24] T. Ohno, M. Akiyoshi, T. Umebayashi, K. Asai, T. Mitsui, M. Matsumura, Preparation of S-doped TiO$_2$ photocatalysts and their photocatalytic activities under visible light, Appl. Catal. Gen. A 265 (2004) 115–121.

[25] E. Roman, J.L. de Segovia, A. Martin-Gago, G. Comtet, L. Hellner, Study of the interaction of SO$_2$ with TiO$_2$ (1 1 0) surface, Vacuum 48 (1997) 597–600.

[26] L.Q. Jing, X.J. Sun, J. Shang, W.M. Cai, Z.L. Xu, Y.G. Du, H.G. Fu, Review of surface photovoltage spectra of nano-sized semiconductor and its applications in heterogeneous photocatalysis, Solar Energy Mater. Solar Cells 79 (2003) 133–151.

[27] L. Gao, S. Zheng, Q.H. Zhang, Nanometer Titanium Oxide Photocatalysis Materials and Application, Chemical Industry Publisher, China, 2002, 43 p. (Chapter 3).

[28] J. Premkumar, Development of super-hydrophilicity on nitrogen-doped TiO$_2$ thin film surface by photoelectrochemical method under visible light, Chem. Mater. 16 (2004) 3980–3987.

[29] S. Sakthivel, M. Janczarek, H. Kisch, Visible light activity and photoelectrochemical properties of nitrogen-doped TiO$_2$, J. Phys. Chem. 108 (2004) 19384–19387.

[30] Y. Tian, H. Notsu, T. Tatsuma, Visible-light-induced patterning of Au– and Ag–TiO$_2$ nanocomposite film surfaces on the basis of plasmon photoelectrochemistry, Photochem. Photobiol. Sci. 4 (2005) 598–601.